7-2011

Identification of Salt-induced Changes in Leaf and Root Proteomes of the Wild Tomato, Solanum chilense

Suping Zhou
Tennessee State University

Roger J. Sauvé
Tennessee State University

Zong Liu
Tennessee State University

Sasikiran Reddy
Tennessee State University

Sarabjit Bhatti
Tennessee State University

Authors

Suping Zhou, Roger J. Sauvé, Zong Liu, Sasikiran Reddy, Sarabjit Bhatti, Simon D. Hucko, Tara Fish, and Theodore W. Thannhauser

Identification of Salt-induced Changes in Leaf and Root Proteomes of the Wild Tomato, *Solanum chilense*

Suping Zhou[1], Roger J. Sauvé, Zong Liu, Sasikiran Reddy, and Sarabjit Bhatti
Department of Agricultural Sciences, School of Agriculture and Consumer Sciences, Tennessee State University, 3500 John A. Merritt Boulevard, Nashville, TN 37209

Simon D. Hucko, Tara Fish, and Theodore W. Thannhauser
Plant, Soil and Nutrition Research Unit, USDA-ARS, Tower Road, Ithaca, NY 14853-2901

ABSTRACT. This article reports salt-induced changes in leaf and root proteomes after wild tomato (*Solanum chilense*) plants were treated with 200 mM NaCl. In leaf tissues, a total of 176 protein spots showed significant changes ($P < 0.05$), of which 104 spots were induced and 72 spots suppressed. Salt-induced proteins are associated with the following pathways: photosynthesis, carbohydrate metabolism, glyoxylate shunt, glycine cleavage system, branched-chain amino acid biosynthesis, protein folding, defense and cellular protection, signal transduction, ion transport, and antioxidant activities. Suppressed proteins belong to the following categories: oxidative phosphorylation pathway, photorespiration and protein translational machinery, oxidative stress, and ATPases. In root tissues, 106 protein spots changed significantly ($P < 0.05$) after the salt treatment, 63 spots were induced, and 43 suppressed by salt treatment. Salt-induced proteins are associated with the following functional pathways: regeneration of *S*-adenosyl methionine, protein folding, selective ion transport, antioxidants and defense mechanism, signal transduction and gene expression regulation, and branched-chain amino acid synthesis. Salt-suppressed proteins are receptor kinase proteins, peroxidases and germin-like proteins, malate dehydrogenase, and glycine dehydrogenase. In this study, different members of proteins were identified from leaf and root tissues after plants were subjected to salt treatment. These proteins represent tissue-specific changes in salt-induced proteomes. When protein expression was compared in the context of metabolic pathways, the branched-chain amino acid biosynthesis, glucose catabolism toward reducing cellular glucose level, and the antioxidant, detoxification, and selective ion uptake and transport were induced in both root and leaf tissues. These changes appear to be associated with salt tolerance in the whole plant.

Excess sodium in arable soil is a widespread and common stress factor in natural and agricultural ecosystems (Food and Agriculture Organization of the United Nations, 2008). Globally, ≈380 million ha, or almost one-third of the farmed land, is affected by salt, water logging, and alkalinity (Flowers et al., 1977; Lambers, 2003; Rengasamy, 2006). Approximately 25% to 30% of the irrigated lands in the United States have crop yields that are negatively affected by high soil salinity levels (Postel, 1989; Wichelns, 1999). In tomato (*Solanum lycopersicum*) production, repeated cultivation on the same land results in the accumulation of residual fertilizers (salts) and contaminants from irrigation water. High salt concentrations affect tomato fruit yield and quality, causing significant losses to many growers (Flowers and Yeo, 1995; Hanson et al., 2009; Maggio et al., 2007). Thus, to maintain tomato production at its current level

without increasing costs, tomato cultivars tolerant to saline soil need to be developed.

Tomato cultivars are generally sensitive to salt stress, whereas some of the wild relative species can grow in high saline conditions. In *Solanum pennellii*, growth was not impaired by high salinity, although plants accumulated more Cl^- and Na^+ ions but less K^+, when grown on saline media (Dehan and Tal, 1978). Transcriptional profiling analysis found that some genes were salt-inducible only in the salt-tolerant wild species *Solanum pimpinellifolium* PI365967 but not in the cultivated 'Money Maker' (Sun et al., 2010). Differences in Na^+ ion accumulation and translocation, proline accumulation, osmotic stress response, antioxidant system, and plant growth have been found in cultivated tomato and wild species (Borsani et al., 2001; Cuartero et al., 2006; Mittova et al., 2002; Sun et al., 2010).

These wild species provide potentially rich sources of genetic traits that can be used to improve salt tolerance of tomato cultivars (Dillon et al., 2007; Tanksley and McCouch, 1997). However, transferring salt tolerance traits from wild species into tomato cultivars has proven to be a very difficult task as a result of the large number of genes involved (Cuartero et al., 2006). Another approach is to use tolerant species to identify gene sequences governing salt tolerance to develop markers for selection of tolerant traits from progenies of hybrids between cultivated and wild species or through the direct genetic modification of single or multiple genes to generate tolerant genotypes (Cuartero et al., 2006; Zhang and Blumwald, 2001).

The wild tomato species, *Solanum chilense*, has a high level of biodiversity (Rick, 1988, 1991; Yañez et al., 1998) and is adapted to a severe salt and drought environment (Bai and Lindhout, 2007; Yañez et al., 1998). *Solanum chilense* LA2747 originated in Alta Azapa, Tarapaca, Chile, and LA1958 in Pampa de la Clemso, Moquequa, Peru. According to the germplasm information found in the Tomato Genetics Resource Center at the University of California (Davis), *S. chilense* LA1958 is drought-tolerant and LA2747 is resistant to salinity. A cross (*S. chilense* LA2747 × LA1958) was made, and the progeny population was used to identify salt-induced changes in leaf and root proteomes. The objective of this study was to identify candidate genes that will be used in functional genomics studies and breeding for salt tolerance in tomato.

Materials and Methods

PLANT GROWTH AND SALT TREATMENT. Seed stocks of *S. chilense* LA 2747 and LA1958 were obtained from the Tomato Genetics Resource Center at the University of California (Davis). Seeds were propagated at Tennessee State University (Nashville). Flowers on LA 2747 plants were hand-pollinated with pollen obtained from LA1958 plants. Seeds were harvested from mature fruits, washed in 10% commercial bleach, air-dried, and stored at 4 °C.

To prepare a standard salt treatment protocol, a hydroponic system was modified from the Megagarden System (Hydrofarm, Seattle, WA). Initially, a salt-tolerant cherry tomato (*S. lycopersicum* var. *cerasiforme* LA 4133) and a salt-sensitive tomato 'Rheinlands Ruhm' LA0535 were treated with 200 mM NaCl in half-strength Hoagland's solution (Hoagland and Arnon, 1950). Plants of 'Rheinlands Ruhm' showed severely stunted vegetative growth, and they did not produce fruits. In contrast, the salt-tolerant cherry tomato produced flowers and fruits of the same quality as plants growing in the control solution (half-strength Hoagland's solution). With these experimental results, the salt treatment system was shown to be effective for testing salt tolerance in tomato.

When progenies of *S. chilense* LA2747 × LA1958 were subjected to salt treatment following the procedures described previously, all plants produced healthy leaves, roots, and flowers (unpublished data). Seeds from the same population were used to identify salt-induced changes in leaf and root proteomes.

For this experiment, seeds were surface-disinfected by soaking in a 50% commercial bleach solution for 10 min followed by three rinses in sterile tap water. Then they were germinated by soaking in sterile tap water for 48 h at 25 °C under slow agitation (50 rpm). Germinating seeds were transplanted to root cubes (Smithers-Oasis, Kent, OH). When seedlings developed two fully expanded leaves, they were transplanted into net pots (3.81 cm wide) filled with hydroteon clay balls and placed in hydroponic tanks, which were modified from the Megagarden System. Each tank was filled with 30 L of solution to a level that submerged the entire root system of each plant.

During the first 3 d of pretreatment incubation, all tanks were filled with half-strength Hoagland's solution. Then, the solution in tanks used for salt treatments was replaced with half-strength Hoagland's solution supplemented with sufficient NaCl to bring its concentration to 200 mM. For the control, the solution was replaced with fresh half-strength Hoagland's solution. All solutions were refreshed every 3 d and maintained at pH 5.8 to

6.0. Twenty plants were grown in each tank; three separate replicates (tanks) were used for the control and the salt treatment. The experiment was conducted in a greenhouse under conditions of 27/23 °C (day/night) temperatures with no supplemental lighting. The experiment was ended after 25 d after a sunny week. Tissues were harvested at 1000 to 1100 HR. Leaf tissues were the leaflets from the top four mature leaves; and the first mature leaf normally started as the second compound leaf from the shoot tip. For the collection of uniform root tissues, the submerged roots were cut with a surgical blade 5 cm from root tips, and the root tip sections from a tank were pooled together to make one sample. All samples were immediately frozen in liquid nitrogen followed by protein extraction as described subsequently.

PREPARATION OF PROTEIN SAMPLES AND TWO-DIMENSIONAL DIFFERENTIAL GEL ELECTROPHORESIS. To extract proteins, frozen tissues were ground into a fine powder and mixed with an acetone solution containing 0.6 M trichloroacetic acid and 32 mM dithiothreitol (Sigma, St. Louis, MO). After an overnight incubation at –20 °C, proteins were precipitated by centrifugation at 10,000 g_n at 4 °C for 10 min. After washing four times in pre-chilled 100% acetone, protein pellets were evaporated to complete dryness in a Thermo Savant SpeedVac (Thermo Fisher Scientific, Waltham, MA) at low heat.

For gel analysis, the protein powder was re-constituted at room temperature in a two-dimensional protein rehydration buffer consisting of 7 M urea, 2 M thiourea, and 2 mM 3-[3-(cholamidopropyl) dimethylammonio]-1-proanesulfonate (Sigma). Soluble proteins were separated by centrifugation at 14,000 g_n for 10 min. Protein concentration was determined using the Bradford Protein Assay Reagent (Bio-Rad, Hercules, CA).

To quantitatively compare the samples using differential gel electrophoresis (DIGE) analysis, three biological replicates were labeled with cyanine dyes Cy3 and Cy5 (GE Healthcare, Piscataway, NJ) according to the manufacturer's instructions. Cy-dye labeled samples were grouped randomly during electrophoresis so that no two Cy3 and Cy5 pairs were run on duplicate gels to eliminate statistical biases (Karp and Lilley, 2007; Karp et al., 2007). A dye swap design was incorporated to control for labeling biases. A combined Cy2-labeled internal standard containing equal amounts of all the protein extractions used in the experiment was used to normalize across the multiple gels (Alban et al., 2003), which greatly reduces variation in gel-to-gel comparisons. The dye:protein ratio for the experiments was 200 pmol dye:50 μg total protein. All analytical gels were run using 50 μg of protein from each labeled sample. A preliminary analysis on a limited number of samples was done to conduct a power analysis to facilitate the design of the large-scale experiment. The pilot study showed that three biological replicates were sufficient to identify differentially expressed proteins with greater than a 1.5-fold change at a statistical power of 0.85 or greater. Therefore, subsequent experiments had three biological replicates per treatment.

Immobilized pH gradient IPG strips (GE Healthcare) of 24 cm in length with nonlinear pH 3.0 to 10.0 gradients were used for isoelectric focusing (IEF). After overnight rehydration at room temperature, the IEF was carried out at 20 °C with voltage starting at 500 V for 4 h and then increasing to 1,000 V for 1 h followed by 8,000 V to reach 70,000 total volt hours on an Ettan IPGphor II unit (GE Healthcare). After IEF, the

proteins were reduced and alkylated (Zhang et al., 2003). Strips were transferred onto 12.52% acrylamide–sodium dodccylsulfate gels, which were prepared using 41.75% (v/v) of protogel (National Diagnostics, Atlanta, GA). The gels were run on a Hoefer SE900 vertical slab gel electrophoresis unit (Hoefer, Holliston, MA) using the following protocol: 20 °C at 20 mA for 30 min and then 50 mA for ≈12 to 13 h until the bromophenol blue front dye migrated to the bottom of the gel (Zhou et al., 2009).

Gels were scanned on the Typhoon 9300 Variable Mode Imager (GE Healthcare) at 100 dots/inch according to the manufacturer's specifications for Cy Dyes (GE Healthcare) and colloidal Coomassie blue- (Invitrogen, Carlsbad, CA) stained gels were imaged with the 632.8 nm helium–neon laser with no emission filter. DIGE gel images were analyzed using Progenesis Samespots Version 3.3 (Nonlinear Dynamics, Newcastle Upon Tyne, UK). All images that passed quality control checks for saturation and dynamic range were cropped to adjust for positional differences in scanning. The alignment procedure was semiautomated. Fifty manual alignment seeds were added per gel (≈12 landmark spots per quadrant) and gels were then autoaligned and grouped according to treatment. Spots (picking lists) were selected as being differentially expressed if they had greater than a 1.5-fold change and past an analysis of variance test at the $P < 0.05$ level.

PROTEIN IDENTIFICATION. For protein identification, a preparative picking gel was run in which 450 μg of protein was loaded. Gel preparation and electrophoresis were carried out following the procedure used for DIGE gels. The picking gels were stained with colloidal blue staining solution (Invitrogen) overnight and destained in distilled, deionized H_2O. Protein spots were manually picked from the gels and digested with trypsin in situ (sequence-grade trypsin; 12.5 ng·mg^{-1}; Promega, Madison, WI) overnight. The resulting peptides were extracted from gel pieces and concentrated with C_{18} ZipTips (Millipore, Bedford, MA). An aliquot of each digest was spotted (along with the matrix 7-mg α-cyano-4-hydroxycinnamic acid in 1.0 mL of 0.1% TFA, 50% CH_3CN, and 1 mM ammonium phosphate) onto a matrix-assisted laser desorption/ionization–mass spectrometry (MALDI-MS) target.

All samples were subjected to MALDI-MS analysis using a 4700 Proteomics Analyzer equipped with tandem time of flight ion optics (Applied Biosystems, Framingham, MA). Before analysis, the mass spectrometer was calibrated, externally, using a six-peptide calibration standard (4700 Cal Mix; Applied Biosystems). Most samples were calibrated internally using the common trypsin autolysis products (at m/z 842.51, 1045.5642, and 2211.1046 Da) as mass calibrants. The external calibration was used as the default if the trypsin autolysis products were not observed in the spectra of the samples. The instrument was operated in the 1-kV positive ion reflector mode. The laser power was set to 4500 for MS and 5200 for MS/MS with collision-induced dissociation off. MS spectra were acquired across the mass range of 850 to 4000 Da. MS/MS spectra were acquired for the 10 most abundant precursor ions provided they exhibited a signal to noise ratio 25 or less. Calibration was external using the known fragments of angiotensin I (monoisotopic mass 1296.6853 Da). A maximum of 2000 laser shots was accumulated per precursor. The MS data were processed using Mascot Daemon (Matrix Science, Boston, MA) to submit searches to Mascot (Version 2.3; Matrix Science). The search parameters used were as follows: tryptic

protease specificity, one missed cleavage allowed, 30 ppm precursor mass tolerance, 0.5-Da fragment ion mass tolerance with a fixed modification of cysteine carbamidomethylation, and a variable modification of methionine oxidation. Spectra were searched against an in-house tomato protein database created by combining 40,000 predicted proteins from the tomato Unigene build 2 (Release 24 Mar. 2009; National Center for Biotechnology Information, Bethesda, MD) and 9000 predicted proteins that to date had been annotated in the tomato genome [Release 3 May 2009; SOL Genomics Network, Ithaca, NY (T.W. Thannhauser, unpublished data)]. The tomato protein database contains 48,988 sequences and 12,750,633 residues. Only peptides that matched with a Mascot score above the 95% confidence interval threshold ($P < 0.05$) were considered for protein identification. Only proteins containing at least one unique peptide (a sequence that had not been previously assigned to a different protein) were considered.

Results

Salt-induced changes in leaf and root proteomes of *S. chilense*

Analysis of DIGE gels of leaf proteins (Fig. 1) identified 176 protein spots that showed significant change ($P < 0.05$), of which 104 spots were induced and 72 spots suppressed by the salt treatment (Fig. 2). Seventy-five protein spots were identified as a single protein with known function.

Fig. 1. The difference gel electrophoresis (DIGE) electropherogram of leaf proteomes of *Solanum chilense* after 25 d of salt treatment. *Solanum chilense* plants were grown in half-strength Hoagland's solution as control and the same solution supplemented with 200 mM NaCl as salt treatment for 25 d. Proteins were labeled with cyanine dyes using the CyDye DIGE Fluors (GE Healthcare, Piscataway, NJ). Proteins from control and treated samples were labeled with Cy3 and Cy5 and an internal control consisting equal amount of all protein extractions was labeled with Cy2. The CyDye-labeled proteins (150 μg total with 50 μg from each of the three labeled samples) were focused on 24-cm Immobiline DryStrips [pH 3 to 10 nonlinear (NL); GE Healthcare (shown on the x-axis)] and then separated on 12.52% acrylamide–sodium dodecyl sulphate gels. The molecular weight markers (Mw) are shown on the y-axis; they are the Cy2-labeled Broad Range Protein Molecular Weight Markers (Bio-Rad, Hercules, CA). Gels were scanned on a Typhoon 9300 Variable Mode Imager (GE Healthcare).

Fig. 2. Pick list image of leaf proteins of *Solanum chilense* after 25 d of salt treatment. Plants were grown in half-strength Hoagland's solution as control and the same solution supplemented with 200 mM NaCl as salt treatment for 25 d. Proteins were labeled with cyanine dyes using the CyDye DIGE Fluors (GE Healthcare, Piscataway, NJ). Proteins from control and treated samples were labeled with Cy3 and Cy5 and an internal control consisting of an equal amount of all protein extractions was labeled with Cy2. The CyDye-labeled proteins (150 μg total with 50 μg from each of the three labeled samples) were focused on 24-cm Immobiline DryStrip [pH 3 to 10 nonlinear (NL), GE Healthcare (shown on the x-axis)] and then separated on 12.52% acrylamide–sodium dodecyl sulphate gels. Gels were scanned on a Typhoon 9300 Variable Mode Imager (GE Healthcare). Gel images were analyzed in Progenesis Samespots program (Version 3.3; Nonlinear Dynamics, Newcastle Upon Tyne, UK). The pick list image shows the identified protein spots (numbered) that had fold change value of above 1.5 (positive or negative) at $P < 0.05$ level in the analysis of variance test. The molecular weight (Mw) on the y-axis is the protein molecular weight standard, and the pH values in the x-axis are the range of isoelectric point value. Arrows point to the spots containing Rubisco activase (spots 785, 809, 832, 897), transketolase (salt-suppressed spots 168, 187; salt-induced spot 242), phosphoglycerate kinase (salt-induced spot 492, salt-suppressed 780), and aldolase (salt-induced spots 569, 585; salt-suppressed spots 559, 563, 931).

For root tissues, 106 protein spots changed significantly ($P < 0.05$) after salt treatment, 63 spots were induced, and 43 suppressed by salt treatment. Forty-three protein spots were found to contain a single protein with a known function (Fig. 3). Some spots contained multiple proteins; these protein spots were excluded from further analysis because quantification of each individual protein could not be determined using data produced in this study.

Functional pathways affected by salt stress in leaf tissues

Proteins identified in leaves were divided into three groups: salt-induced (Table 1), salt-suppressed group (Table 2), and proteins identified in multiple isoforms following differential expression changes after the salt treatment (Table 3).

Salt-induced proteins in leaf tissues. Salt-induced proteins were associated with 11 functional categories (Table 1) affecting photosynthesis and carbohydrate metabolism, glyoxylate shunt, amino acid metabolism, protein folding, defense, and cellular protection mechanisms.
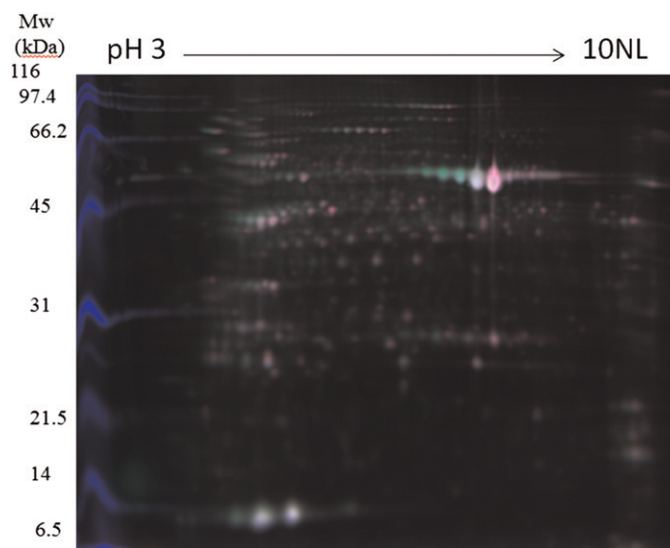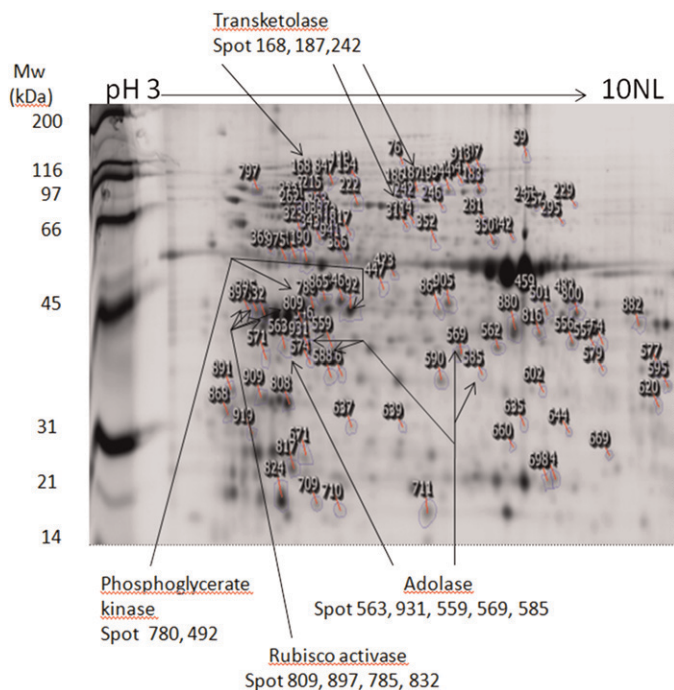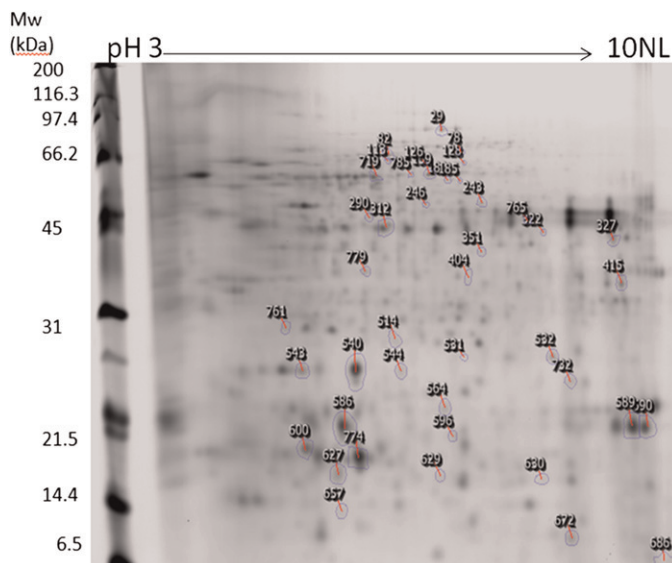

Fig. 3. The difference gel electrophoresis (DIGE) electropherogram of root proteomes of *Solanum chilense* after 25 d of salt treatment. Plants were grown in half-strength Hoagland's solution as control and the same solution supplemented with 200 mM NaCl as salt treatment for 25 d. Root proteins were labeled with cyanine dyes using the CyDye DIGE Fluors (GE Healthcare, Piscataway, NJ). Proteins from control and treated samples were labeled Cy3 and Cy5 and an internal control consisting equal amount of all protein extractions was labeled with Cy2. The CyDye-labeled proteins (150 μg total with 50 μg from each of the three labeled samples) were focused on 24-cm Immobiline DryStrip [pH 3 to 10 nonlinear (NL), GE Healthcare] and then separated on 12.52% acrylamide–sodium dodecyl sulphate gels. Gels were scanned on a Typhoon 9300 Variable Mode Imager (GE Healthcare). Gel images were analyzed in Progenesis Samespots program (Version 3.3; Nonlinear Dynamics, Newcastle Upon Tyne, UK). The numbered spots each contained single protein, which was identified using matrix-assisted laser desorption/ionization-mass (MALDI) spectrometry on a 4700 Proteomics Analyzer (Applied Biosystems, Framingham, MA). The molecular weight (Mw) on the y-axis indicates molecular weight of protein standards, and the pH values on the x-axis refer to the range of isoelectric point value.

Photosynthesis consists of two steps, the light-dependent reaction centers and the carbon fixation cycle (the Calvin cycle). For the light-dependent reaction, three types of proteins were induced, the chlorophyll a/b-binding proteins (LHCI type III, LHCII type III, and CP26), the PSII oxygen-evolving complex 23 protein, and the ferredoxin-NADP+-reductase, which is a component of the PSI reaction center. An additional function of ferredoxin-NADP+ reductase is that it participates in the cellular defense mechanism against oxidative damage (Lee et al., 2006). Three proteins in the carbon fixation reactions were induced, including glyceraldehyde 3-phosphate dehydrogenase (GAPDH), ribulose-phosphate 3-epimerase, and ribose 5-phosphate isomerase. Two proteins, sucrose synthase and glucose-1-phosphate uridylyltransferase, associated with carbohydrate metabolism were identified. Sucrose synthase is involved in soluble sucrolytic activities and its accumulation was also enhanced by salt stress in the leaves of tomato 'Pera' (Balibrea et al., 2000).

The glyoxylate bypass, or glyoxylate shunt, occurs in glyoxysomes. Activation of this pathway can reduce NADH production as well as allow a partial Krebs cycle to function to generate intermediates for anabolic reactions (e.g., amino acid biosynthesis) without the decarboxylation steps. Activation of the glyoxylate cycle by salt stress was also observed in *Debaryomyces hansenii* (Sánchez et al., 2008). Low seed germination rate under drought and NaCl treatments was

Table 1. Salt-induced proteins in leaves of *Solanum chilense.*

Spot no.	Fold change value[z]	P[y]	UniGene code[x]	Putative protein	Peptide sequence hit[w]	Protein score[v]
Photosynthetic structure						
671	1.8	3.94E-04	SGN-U581495	LHCI type III	QYFLGLEK; FAMLGAAGAIAPEILGK; GLGGSGDPAYPGGPLFNPLGFGKDEK	46
824	1.5	4.04E-04	SGN-U581281	PSII oxygen-evolving complex 23	TADGDEGGKHQLITATVNDGK; YEDNFDSTSNLIVAVTPTDK	62
311	1.9	0.002	SGN-U579731	LHCII type III	ALEVIHGR; VDFKEPVWFK	65
229	2	0.002	SGN-U570980	Chloroplast outer envelope protein	AEYAVDHNSGTGAVFFR; LGNVCEGNTQYPVVR; GGRPTLASIQPGGTVSFEHR	39
817	1.8	0.001	SGN-U580870	Chlorophyll A-B binding protein CP26	YQAYELIHAR; LHPGGPFDPLGLAK; LHPGGPFDPLGLAK	237
808	1.6	0.001	SGN-U580023	Extrinsic subunit of PSII	QLVASGKPESFSGEFLVPSYR; GTGTANQCPTIEGGVGSFAFKPGK; DGIDYAAVTVQLPGGER	473
590	1.7	0.005	SGN-U581081	Ferredoxin–NADP(+) reductase	DPNATVIMLATGTGIAPFR; GVCSNFLCDLKPGAEVK; DPNATVIMLATGTGIAPFR	860
868	2	0.003	SGN-U567981	Plastid-lipid associated protein PAP	GDAGSVFVLIK; QLADSFYGTNR; ISPGGVAVVDEEPPKEPSEIELLK	161
Calvin cycle						
554	1.5	0.004	SGN-U579788	Glyceraldehyde 3-phosphate dehydrogenase (GAPDH)	GILGYTEDDVVSTDFVGDNR	57
557	1.6	0.006	SGN-U579788	GAPDH	AVTVFGFR; GILGYTEDDVVSTDFVGDNR	57
864	2	7.96E-05	SGN-U579788	GAPDH	AVSLVLPQLK; GTMTTTHSYTGDQR	43
556	1.8	1.65E-04	SGN-U579788	GAPDH	GILGYTEDDVVSTDFVGDNR; VPTVDVSVVDLTVR; DAPMFVVGVNEK	117
905	1.9	0.002	SGN-U579788	GAPDH	GTMTTTHSYTGDQR	127
595	2.1	0.01	SGN-U580678	Ribulose-phosphate 3-epimerase	AGADIVSVHCEQSSTIHLHR; AVEQAGCDWIHVDVMDGR	285
919	1.7	0.012	SGN-U570787	Ribose 5-phosphate isomerase	LQELFKEEGVDAK; LGELLSSGQLTNIVGVPTSK; SGMVLGLGTGSTAAFVVAK	176
Carbohydrate metabolism						
295	2.1	0.002	SGN-U579955	Sucrose synthase	ISGTDIPR	31
423	2.2	0.005	SGN-U579867	Glucose-1-phosphate uridylyltransferase	YANSNIDIHTFNQSQYPR	111
Glyoxylate shunt in glyoxysomes						
257	3	0.003	SGN-U583127	Formate-tetrahydrofolate ligase	AYVTENLGLVEAGCVNLAR; YSGLKPQCAIIVATVR; GAPSGFILPIR	83
577	1.6	0.018	SGN-U574919	Glyoxisomal malate dehydrogenase	TGAEEVYQLGPLNEYER; ANTFVAEVLGLDPR; VAILGAAGGIGQPLAMLMK	139
Glycine cleavage system						
637	1.5	0.009	SGN-U578979	Dihydrolipoamide dehydrogenase	LTLEPAAGGEQTTLEADVVLVSAGR; FPFLANSR; EGHVDYDLVPGVCYTHPEVASVGK	196
350	1.6	0.015	SGN-U578979	Dihydrolipoamide dehydrogenase	FPFLANSR; LTLEPAAGGEQTTLEADVVLVSAGR; EGHVDYDLVPGVCYTHPEVASVGK	196
800	2	0.002	SGN-U579550	Aminomethyltransferase	VTDDHIYLVVNAGCR; VLDINGAPCFLTR; MYFGEFR	593

292

J. Amer. Soc. Hort. Sci. 136(4):288–302. 2011.

Table 1. Continued.

Spot no.	Fold change value[z]	P[y]	UniGene code[x]	Putative protein	Peptide sequence hit[w]	Protein score[v]
913	1.6	0.004	SGN-U580312	Glycine dehydrogenase	EYAAYPAPWLR; ETPFLTHQIFNSYHTEHELLR; LGTVEVQDLPFFDTVK	267
107	2.5	1.90E-04	SGN-U580312	Glycine dehydrogenase	ETPFLTHQIFNSYHTEHELLR; EYAAYPAPWLR; NLLENPAWYTQYTPYQAEISQGR	267
Amino acid biosynthesis						
941	1.7	0.006	SGN-U578934	Glutamate decarboxylase	GSSQVIAQYYQLIR	56
839	2.6	8.48E-04	SGN-U572725	Ketol-acid reductoisomerase	GILLGAVHGIVESLFR; QIGVIGWGSQGPAQAQNLR; EINGAGINASFAVHQDIDGR	75
281	2.1	7.55E-04	SGN-U581636	S-adenosylhomocysteinase	RAFVPSPIAAAWLR	30
Cellular protection						
797	2	5.54E-04	SGN-U579041	Heat shock protein 81-2	RAPFDLFDTK; GIVDSEDLPLNISR; KPEEITKEEYAAFYK	87
263	1.8	0.01	SGN-U583105	Heat shock protein 70	AVVTVPAYFNDAQR	27
226	2.4	2.85E-04	SGN-U567765	Peptidyl-prolyl cis-trans isomerase	SDGVEFTVQDGHFCPALAK; VQLTVKPQYGFGEK; KGEAALLTIAPEYAFGSSESK	61
231	3	3.93E-04	SGN-U567765	Peptidyl-prolyl cis-trans isomerase	SDGVEFTVQDGHFCPALAK; VQLTVKPQYGFGEK	61
669	1.9	3.37E-04	SGN-U574403	Osmotin-like protein	ANLLESCPAVLQFR	47
323	2.6	3.39E-04	SGN-U577228	Betaine-aldehyde dehydrogenase	LIIQETIAPQFLAR	52
343	2	0.006	SGN-U580690	Ultraviolet-B and ozone regulated protein	NFSEPEDLSAYDGLELR	30
709	2.2	0.002	SGN-U578588	Superoxide dismutase	RPDYISIFMEK; DFGSYDTFVK	87
Signal transduction						
660	1.5	0.017	SGN-U579951	Ras-related GTP-binding protein	SNYNFEKPFLYLAR; KYEPTIGVEVHPLDFFTNCGK; NLQYYEISAK	112
Cytoskeletal system						
846	1.7	0.002	SGN-U577711	Actin 7 (ACT7)/actin 2	NYELPDGQVITIGAER; AVFPSIVGRPR; VAPEEHPVLLTEAPLNPK	264
Ion transporters						
262	1.8	4.72E-04	SGN-U578206	Vacuolar H+-ATPase	NIIHFYNLANQAVER; EASIYTGITIAEYFR; YSNSDTVVYVGCGER	72

[z]Fold change value is the ratio of the normalized volume of the same spot in the condition of salt-treated (growing in half-strength Hoagland's solution containing 200 mM NaCl for 25 d) versus control (half-strength Hoagland's solution). For example, a value of 2.0 represents a twofold increase, whereas –2.0 represents a twofold decrease from treated to control conditions.

[y]Probability value in an analysis of variance test of difference between treated and untreated samples each with three biological replicates.

[x]Code for each gene in the SOL Genomics Network (Ithaca, NY) database.

[w]Peptide sequence used in Mascot (Version 2.3; Matrix Science, Boston, MA) search to identify the protein in the protein database.

[v]Protein score is derived from the ion scores. An ion's score is based on the calculated probability that the observed match between the experimental data and the database sequence is a random event. The reported score is –10Log (P). For a search containing a small number of queries, the protein score is the sum of the highest ions score for each unique sequence, excluding the scores of duplicate matches. A correction (usually very small) is applied to reduce the contribution of low-scoring random matches.

accompanied with reduced activity of glyoxylate cycle in *Pinus pinea* (Sidari et al., 2008). Two enzymes in the glyoxylate shunt were identified, formate-tetrahydrofolate ligase (spot 257) and glyoxysomal malate dehydrogenase (spot 577).

The glycine cleavage complex is composed of four proteins: the T-protein (aminomethyltransferase), P-protein (glycine dehydrogenase), L-protein (dihydrolipoyl dehydrogenase), and H-protein. This multienzyme system is triggered in response

Table 2. Salt-suppressed proteins in leaves of *Solanum chilense*.

Spot no.	Fold change value[z]	P[y]	UniGene code[x]	Predicted protein	Peptide sequence hit[w]	Protein score[v]
Oxidative phosphorylation						
386	−1.5	0.004	SGN-U569105	Ubiquinol-cytochrome C reductase	LNSTVLEEFVAANYTAPR; VSATEEPKPVYVGGDYR; QLLTYGER	40
Photorespiration						
909	−1.8	0.003	SGN-U569247	Phosphoglycolate phosphatase	ENPGCLFIATNR; LIDGVPETLDLLR; IQYATLCIR	139
501	−2.1	0.003	SGN-U586528	Hydroxypyruvate reductase	VLDINGAPCFLTR; MYFGEFR; SLLALQGPLAAPVLQYLTK	418
882	−1.9	0.002	SGN-U578941	Glycolate oxidase	IPVFLDGGVR; LAVQAGAAGIIVSNHGAR; FVLPPFLTLK	64
Protein translation						
865	−1.5	0.002	SGN-U577523	Elongation factor Tu/EF-Tu	KYDEIDAAPEER; GITINTATVEYETENR; QTELPFLMAIEDVFSITGR	278
Calvin cycle						
571	−1.9	8.44E-04	SGN-U574431	Sedoheptulose-1,7-bisphosphatase	MFSPGNLR; EQVAAAMGIFGPR; FEETLYGSSR	113
Myo-inositol sysnthesis						
307	−2.8	1.05E-04	SGN-U577578	Inositol-3-phosphate synthase	DKVQQANYFGSLTQASTIR	53
Purine metabolism, selenoamino acid metabolism, and sulfur metabolism						
447	−1.9	4.74E-04	SGN-U573423	Sulfate adenylyltransferase 1	NADAVFAFQLR; INAGANFYIVGR; LVELFVEESQR	55
Vesicle transport						
546	−1.8	0.004	SGN-U588197	Vesical transport v-SNARE 12 (VTI12)	ISPSPIIR	26
ATP synthesis						
602	−1.8	9.48E-04	SGN-U585234	Chloroplast-encoded gene ATP synthase	DVNEQDVLLFIDNIFR; DSVGQPINVACEVQQLLGNNR; AHGGVSVFGGVGER	836
811	−2	9.89E-04	SGN-U585664	ATP synthase beta chain 2	IPSAVGYQPTLATDLGGLQER; EAPAFVEQATEQQILVTGIK	351
390	−1.7	0.001	SGN-U585234	Chloroplast-encoded gene ATP synthase	DSVGQPINVACEVQQLLGNNR; VALVYGQMNEPPGAR; DVNEQDVLLFIDNIFR	83
369	−1.8	0.002	SGN-U584963	ATPA | ATPase alpha subunit	EAYPGDVFYLHSR; IAQIPVSEAYLGR; TTKPQFQEIISSTK	135

[z]Fold change value is the ratio of the normalized volume of the same spot in the condition of salt-treated (growing in half-strength Hoagland's solution containing 200 mM NaCl for 25 d) versus control (half-strength Hoagland's solution). For example, a value of 2.0 represents a twofold increase, whereas −2.0 represents a twofold decrease from treated to control conditions.

[y]Probability value in an analysis of variance test of difference between treated and untreated samples each with three biological replicates.

[x]Code for each gene in the SOL Genomics Network (Ithaca, NY) database.

[w]Peptide sequence used in Mascot (Version 2.3; Matrix Science, Boston, MA) search to identify the protein in the protein database.

[v]Protein score is derived from the ion scores. An ion's score is based on the calculated probability that the observed match between the experimental data and the database sequence is a random event. The reported score is −10Log (P). For a search containing a small number of queries, the protein score is the sum of the highest ions score for each unique sequence, excluding the scores of duplicate matches. A correction (usually very small) is applied to reduce the contribution of low-scoring random matches.

to high concentrations of the amino acid glycine. The salt treatment induced three of the component proteins in that system; these include dihydrolipoamide dehydrogenase (spots 350, 637), aminomethyltransferase (spot 800), and glycine dehydrogenase (spots 107, 913).

Three enzymes associated with the metabolism of amino acids were identified. They are glutamate decarboxylase, ketol-acid reductoisomerase, and S-adenosylhomocysteinase. Glutamate decarboxylase or glutamic acid decarboxylase is an enzyme in the γ-aminobutyric acid (GABA) shunt contributing

Table 3. Multiple isoform proteins following differential expression changes in leaves of *Solanum chilense* after salt treatment.

Spot no.	Fold change value[z]	P[y]	UniGene code[x]	Putative protein	Peptide sequence hit[w]	Protein score[v]
Germin protein						
562	3.1	2.59E-04	SGN-U580695	Germin-like protein 1	VTADDFVFSGLAATGK; AAVTPAFAPQFPGVNGLGISMAR	48
711	−1.5	0.001	SGN-U566992	Germin-like protein (GER1)	AAVTPAFAAQFPGLNGLGLSAAR	94
Phosphoglycerate kinase						
492	2.6	3.94E-04	SGN-U580583	Phosphoglycerate kinase	ADLNVPLDDSQNITDDTR; KLASLADLYVNDAFGTAHR; AQGLSVGSSLVEEDKLELATSLLEK	1158
780	−2	3.30E-04	SGN-U580583	Phosphoglycerate kinase	FLKPSVAGFLLQK; LASLADLYVNDAFGTAHR; ADLNVPLDDSQNITDDTR	1158
Rubisco activase						
809	1.6	0.001	SGN-U577570	Rubisco activase	IVDSFPGQSIDFFGALR; SFQCELVFR; VPIIVTGNDFSTLYAPLIR	689
897	−4.1	0.004	SGN-U577570	Rubisco activase	VPIIVTGNDFSTLYAPLIR	1053
785	−3.1	5.97E-04	SGN-U577570	Rubisco activase	GGVVALVEGLR; GFVPFSQISTK; SIQYDLAWER	75
832	−2.2	6.45E-04	SGN-U577570	Rubisco activase	IVDSFPGQSIDFFGALR; GLYDNTSDDQQDIAR; FYWAPTR	689
Transketolase						
168	−2.5	5.94E-05	SGN-U578988	Transketolase	ALPTYTPESPADATR; QKLPQLAGTSIEGAAK; NLSQQNLNALAK	288
187	−3.1	6.83E-05	SGN-U578988	Transketolase	ALPTYTPESPADATR	288
242	1.7	0.01	SGN-U578988	Transketolase	NPYWFNR; NNLGWPYEPFHVPEDVK; IPGHPENFETPGVEVTTGPLGQGIANAVGLAVAEK	350
Adolase						
569	1.8	5.55E-04	SGN-U578125	Aldolase	SAAYYQQGAR; GLVPLAGSNNESWCQGLDGLASR; EAAWGLAR	822
585	1.6	0.005	SGN-U578125	Aldolase	SAAYYQQGAR; YAAISQDNGLVPIVEPEILLDGEHNIDR; GLVPLAGSNNESWCQGLDGLASR	822
931	−2.3	0.004	SGN-U580022	Aldolase	SAAYYQQGAR; RLDSIGLENTEANR; ATPEQVADYTLK	135
559	−1.7	0.001	SGN-U580022	Aldolase	SAAYYQQGAR; ATPQQVADYTLSLLR	71
563	−1.6	0.003	SGN-U581552	Aldolase	LNASQSLELSFIVAEITK	180
Peptidase						
944	−1.9	0.015	SGN-U562601	Peptidase M1	IGGGVNIPR	80
186	−3.1	0.002	SGN-U562601	Peptidase M1	IGGGVNIPR	80
215	−2.5	0.003	SGN-U562601	Peptidase M1	IGGGVNIPR	80
313	−1.9	0.001	SGN-U562601	Peptidase M1	IGGGVNIPR	80
588	−2.8	0.001	SGN-U562601	Peptidase M1	IGGGVNIPR	80
190	−2.5	1.10E-04	SGN-U562601	Peptidase M1	IGGGVNIPR	80
208	−1.5	0.006	SGN-U562601	Peptidase M1	IGGGVNIPR	80
76	1.5	0.002	SGN-U562601	Peptidase M1	IGGGVNIPR	80
59	2	0.001	SGN-U562601	Peptidase M1	IGGGVNIPR	80

[z]Fold change value is the ratio of the normalized volume of the same spot in the condition of salt-treated (growing in half-strength Hoagland's solution containing 200 mM NaCl for 25 d) versus control (half-strength Hoagland's solution). For example, a value of 2.0 represents a twofold increase, whereas −2.0 represents a twofold decrease from treated to control conditions.

[y]Probability value in an analysis of variance test of difference between treated and untreated samples each with three biological replicates.

[x]Code for each gene in the SOL Genomics Network (Ithaca, NY) database.

[w]Peptide sequence used in Mascot (Version 2.3; Matrix Science, Boston, MA) search to identify the protein in the protein database.

[v]Protein score is derived from the ion scores. An ion's score is based on the calculated probability that the observed match between the experimental data and the database sequence is a random event. The reported score is −10Log (P). For a search containing a small number of queries, the protein score is the sum of the highest ions score for each unique sequence, excluding the scores of duplicate matches. A correction (usually very small) is applied to reduce the contribution of low-scoring random matches.

J. Amer. Soc. Hort. Sci. 136(4):288–302. 2011.

295

to the carbon: nitrogen balance. GABA is a metabolite produced in response to stress; it is also used as a signal molecule to activate alteration in metabolic pathways of plants (Bouché and Fromm, 2004; Xing et al., 2007).

The peptidyl-prolyl cis-trans isomerase (PPIase) plays an important role in de novo folding of nascent proteins as well as refolding of proteins where the disulfide bonds are left intact in the unfolded polypeptide chain (Göthel and Marahiel, 1999; Schonbrunner and Schmid, 1992). Heat shock proteins (HSPs) function as molecular chaperones and play a critical role in protein folding and intracellular trafficking of proteins. Both PPIase (spots 226, 231) and HSPs (spots 263, 797) were induced by the salt treatment.

The superoxide dismutase (SOD) (spot 709) provides defense against oxidative stress by repairing cellular damages from accumulation of superoxide molecules. SOD activity was significantly higher in leaves of the tolerant *S. pennellii* than in the sensitive cultivated tomato when plants were exposed to salt treatment (Koca et al., 2006). The betaine-aldehyde dehydrogenase catalyzes the biosynthesis of osmoprotectant glycine betaine under osmotic stress. Together with the osmotin-like protein (spot 669, 1.9-fold), the induction of betaine-aldehyde dehydrogenase (spot 323) may enhance the cellular capacity against osmotic stress in leaves of *S. chilense*. The vacuolar H+-ATPase (spot 262) could be a transporter for intracellular compartmentalization of toxic ions.

SALT-SUPPRESSED PROTEINS IN LEAF TISSUES. Salt-suppressed proteins were classified into nine groups (Table 2). In the oxidative phosphorylation pathway, ubiquinol-cytochrome C reductase (spot 386) was identified. This pathway is highly efficient in releasing energy but produces reactive oxygen species (ROS) during electron transport in the mitochondria (Zsigmond et al., 2008). The sedoheptulose-1, 7-bisphosphatase (spot 571) in the Calvin cycle was also suppressed. Three proteins in the photorespiration pathway were identified: phosphoglycolate phosphatase, hydroxypyruvate reductase, and glycolate oxidase. The vesicle soluble NSF attachment protein receptor VTI1b (spot 546) for intracellular trafficking and four ATP synthase proteins were suppressed by salt stress.

PROTEINS IDENTIFIED IN MULTIPLE SPOTS AFTER DIFFERENTIAL CHANGING PATTERNS AFTER THE SALT TREATMENT. Proteins in this group were identified as multiple isoforms in separate protein spots, which changed differently in response to the salt treatment (Table 3; Fig. 2). For the two germin-like proteins, the SGN-U580695 was increased and SGN-U566992 suppressed. These two genes are located in separate loci (SOL Genomics Network, 2011). Salt stress could have affected, in a different manner, the protein expression (synthesis) or turnover (stability) of these two isoenzymes.

Phosphoglycerate kinases (PGK) were identified in two spots, one with higher pI (spot 492, twofold) and one of lower pI (spot 780, –twofold). Three aldolase protein spots (spots 559, 563, 931) were suppressed and two spots (spots 569, 585) induced. Transketolase were identified in three spots, one induced (spot 242) and two suppressed (spots 168, 187).

Rubisco activase is a stromal protein usually present in two isoforms of 41 to 43 kDa and 45 to 46 kDa that arise from one alternatively spliced transcript. The larger isoform is regulated by the redox status in the stroma (Zhang et al., 2002); it may play an important role in photosynthetic acclimation to moderate heat stress in vivo. The smaller isoform plays a major role in maintaining Rubisco initial activity under normal conditions (Wang et al., 2010). In *S. chilense* leaves, three spots (spots 785, 832, 897) containing the larger isoforms of Rubisco activase were suppressed; only the smaller isoform protein (spot 809) was induced. The contrasting expression pattern between these two isoforms suggests that they might play very different roles in maintaining photosynthesis under high salt conditions.

Functional pathways affected by salt stress in root tissues

Proteins identified from roots were divided into two groups, salt-induced proteins (Table 4) and salt-suppressed proteins (Table 5).

SALT-INDUCED PROTEINS IN ROOTS. As shown in Table 4, salt stress induced the expression of enzymes in the S-adenosylmethionine (SAM) regeneration pathway. Three identified proteins include 5-methyltetrahydropteroyltriglutamate-homocysteine methyltransferase in two spots (spots 29 and 185), S-adenosylmethionine synthetase 1 (spot 544, 2.9-fold), and S-adenosylhomocysteinase (spot 309, 1.4-fold).

Two protein isoforms of the peptidyl-prolyl cis-trans isomerase/cyclophilins (CYPs) (spot 78, twofold; spot 590, 2.6-fold) as well as the FK506-binding protein 2-1 (spot 672, 1.7-fold) were induced by the salt treatment. FK506 binding proteins and CYPs all belong to the PPIase superfamily, which is involved in protein folding and formation of functional structure. PPIase proteins participate in signal transduction, trafficking, assembly and disassembly of proteins, and cell cycle regulation (Göthel and Marahiel, 1999; Ivery, 2000). Expression of PPIase is associated with a plant's response to environmental stresses (Ahn et al., 2010).

The toxicity of salts to plant cells is greatly affected by the ionic concentration in the cytoplasmic space. Four proteins associated with inter- and intracellular ion transportation were induced. These included two ATPase subunits (spots 159 and785), one porin protein for selective crossmembrane ion transportation (spot 415, 1.5-fold), and one vesical transport protein (spot 629, 1.8-fold).

Salt affected the expression of proteins associated with signal transduction and gene transcriptional and translational regulation. Serine/threonine protein kinases are known to act as sensors of environmental signals and they also play key roles in the regulation of cell growth and proliferation (Nigg, 1993). One serine/threonine protein kinase protein was induced by the salt treatment (spot 589, 2.1-fold). Expression of the protein may trigger a plant response to salt stress. Three proteins that could regulate gene expression were also induced. These include a zinc-finger transcription factor protein (spot 290, 1.9-fold), a cold-shock DNA binding protein (spot 128, 1.8-fold), and a translationally controlled tumor family protein (spot 627, 1.8-fold).

For the antioxidant system, two isoforms for SOD (spot 543, 774) were induced along with a thoredoxin H-type protein (spot 657) and one germin-like protein (spot 586).

For proteins affecting amino acid metabolism, the keto-acid reductoisomerase (spot 113, 2.2-fold) was induced. This enzyme is a key enzyme in branched-chain amino acid synthesis. Additional salt-induced enzymes included cytosolic malic enzyme (spot 82, 3.4-fold), which catalyzes the reaction of converting malate into pyruvate and NADPH and UDP-glucose pyrophosphorylase (spot 126, 1.9-fold) for the conversion of glucose to UDPG. Several enzymes in the glycolytic pathway were identified, including triose phosphate isomerase (spot 540, 2.7-fold), GAPDH (spot 564, 1.7-fold), and enolase (spot 719,

Table 4. Salt-induced proteins in roots of *Solanum chilense*.

Spot no.	Fold change value[z]	P^y	UniGene code[x]	Putative protein	Peptide sequence hit[w]	Protein score[v]
S-adenosylmethionine (SAM) regeneration						
29	7.2	0.002	SGN-U577720	5-methyltetrahydropteroyltriglutamate–homocysteine methyltransferase	YGAGIGPGVYDIHSPR	72
185	3.3	2.96E-04	SGN-U577720	5-methyltetrahydropteroyltriglutamate–homocysteine methyltransferase	GVTAFGFDLVR; YGAGIGPGVYDIHSPR	72
544	2.9	0.003	SGN-U590701	S-adenosylmethionine synthetase 1	TIVANGLAK	177
309	1.4	0.008	SGN-U581636	S-adenosylhomocysteinase	ATDVMIAGK	63
Protein folding						
672	1.7	0.008	SGN-U584539	FK506-binding protein 2-1	LTDGTVFDSSYER	36
590	2.6	0.002	SGN-U577630	peptidyl-prolyl cis-trans isomerase/cyclophilins	VFFDLTIGGAPAGR; HVVFGQVVEGMDVIK; VVMELFADTTPK; VVMELFADTTPK; FNDENFVKK	131
78	2	0.003	SGN-U592479	Peptidyl-prolyl cis-trans isomerase/cyclophilins	VVMELFADTTPK; VFFDLTIGGAPAGR; VFFDLTIGGAPAGR; VVMELFADTTPK; HVVFGQVVEGMDVIK	96
Transporters						
785	1.9	0.004	SGN-U577869	ATP synthase subunit alpha	EVAAFAQFGSDLD; AATQALLNR	32
159	2.2	6.97E-04	SGN-U577869	ATPase subunit 1	EAFPGDVFYLHSR; ISHFYTNFQVDEIGR; QILVIYAAVNGFCDR	101
415	1.5	7.71E-04	SGN-U570210	Porin	FSITTYSPTGVVITSSGSK; KGDLFLADVNTQLK	53
629	1.8	0.011	SGN-U588197	Vesical transport v-SNARE 12	ISPSPIIR	26
Proteases						
183	2.9	1.67E-04	SGN-U562601	Peptidase M1 family protein	IGGGVNIPR	80
351	2.1	0.006	SGN-U562601	Peptidase	IGGGVNIPR	80
246	2.8	0.003	SGN-U562601	Peptidase M1 family protein	IGGGVNIPR	80
Signaling transduction, gene transcription, and translation regulators						
290	1.9	0.006	SGN-U573046	Zinc finger protein family	VLLLRIR	18
128	1.8	0.002	SGN-U579937	Cold-shock DNA-binding family protein	SLAEGEDVEYQIESGSDGR	30
589	2.1	0.005	SGN-U586864	Serine/threonine protein kinase	CFETEVKR	31
627	1.8	0.003	SGN-U581240	Translationally controlled tumor family protein	AIGGQSATIASR	42
600	1.6	0.002	SGN-U585835	Glycyl-tRNA synthetase	VAMEMKADLC	29
Oxidative stress and defense						
543	1.7	0.012	SGN-U579086	Superoxide dismutase [Mn]	VIIFAVPGAFTPTCSMK	181
774	2	0.004	SGN-U581590	Superoxide dismutase [Cu-Zn] 2	QIPLTGPQSIIGR; EHGAPEDEVR; QIPLTGPQSIIGR	134
586	4.3	1.98E-04	SGN-U580695	24K germin-like protein	VFFKTLK	30
657	1.6	0.001	SGN-U578414	Thioredoxin H-type 1 (TRX-H-1)	FIAPILADIAK	499
243	1.8	4.84E-04	SGN-U578441	Pathogenesis-related protein 10	GDHVVSEEEHNVGK	44
596	2.3	0.015	SGN-U570975	Membrane protein	VDGFCGLK	
Branched chain amino acid biosynthesis						
113	2.2	0.004	SGN-U572728	Ketol-acid reductoisomerase	FDYNLTQQALVAVDN;NTPINR; EVNGAGINSSFAVHQDIDGR; VTLAGNDEYIVR	70

J. Amer. Soc. Hort. Sci. 136(4):288–302. 2011.

297

Table 4. Continued.

Spot no.	Fold change value[z]	P[y]	UniGene code[x]	Putative protein	Peptide sequence hit[w]	Protein score[v]
Polysaccharide synthesis						
126	1.9	0.005	SGN-U579867	UDP-glucose pyrophosphorylase	ATSDLLLVQSDLY;TLTDEGYVIR	60
Malate partitioning and NADPH production						
82	3.4	6.21E-05	SGN-U577798	Cytosolic NADP-malic enzyme	RPQGLYISLNEK; AVKPTVLIGTSGTGR;	149
322	2.4	7.03E-04	SGN-U574588	Isocitrate dehydrogenase (NADP+)	SKYEEAGIWYEHR	37
Glycolysis						
540	2.7	4.06E-04	SGN-U579400	Triose phosphate isomerase cytosolic isoform-like	TFFVGGNWK; VIACVGETLEQR; ESADVKVDIDAGR	158
564	1.7	0.002	SGN-U580213	NADPH	GILGYTEDDVVSTDFVGDSR; VVSWYDNEWGYSSR	47
719	2.4	3.01E-04	SGN-U579393	Enolase	IEEELGSEAVYAGASFR	198

[z]Fold change value is the ratio of the normalized volume of the same spot in the condition of salt-treated (growing in half-strength Hoagland's solution containing 200 mM NaCl for 25 d) versus control (half-strength Hoagland's solution). For example, a value of 2.0 represents a twofold increase, whereas –2.0 represents a twofold decrease from treated to control conditions.

[y]Probability value in an analysis of variance test of difference between treated and untreated samples each with three biological replicates.

[x]Code for each gene in the SOL Genomics Network (Ithaca, NY) database.

[w]Peptide sequence used in Mascot (Version 2.3; Matrix Science, Boston, MA) search to identify the protein in the protein database.

[v]Protein score is derived from the ion scores. An ion's score is based on the calculated probability that the observed match between the experimental data and the database sequence is a random event. The reported score is –10Log (P). For a search containing a small number of queries, the protein score is the sum of the highest ions score for each unique sequence, excluding the scores of duplicate matches. A correction (usually very small) is applied to reduce the contribution of low-scoring random matches.

2.4-fold). Isocitrate dehydrogenase (spot 322, 2.4-fold), which is involved in the conversion of isocitrate into NADPH and 2-oxoglutarate, was also induced.

SALT-SUPPRESSED PROTEINS IN ROOTS. Salt-suppressed proteins in root tissues were divided into seven groups (Table 5). The protease group contained two proteins, one proteasome (spot 732, –1.5-fold) and one peptidase M1 family protein (spot 765, –1.8-fold). The transporter SNARE 2 protein was identified in two spots (spots 514 and 630). The oxidative stress group contained one peroxidase isoform protein (spot 327, –1.6-fold) and one germin-like protein (spot 532, –2.3-fold). A leucine-rich repeat transmembrane protein kinase (spot 686, –3.1-fold), a malate dehydrogenase (decarboxylating) in the tricarboxylic acid cycle (spot 312, –1.6-fold), and a glucose phosphomutase (spot 531, –3.7-fold) were all suppressed under salt treatment.

Discussion

REGULATION OF THE ANTIOXIDANT SYSTEM BY SALT TOLERANCE. Salt stress activates the generation of ROS molecules that are harmful to plant cells at high concentrations. To reduce ROS damage, higher plants have developed a complex scavenging system consisting of enzymatic and non-enzymatic components. The ultimate capacity of a plant's antioxidant system has a significant impact on its ability to cope with abiotic and biotic stresses, including salt (Pang and Wang, 2008). In *S. chilense*, salt-induced SOD in both leaf and root tissues and ferridoxin-NADP+ reductase in leaves. Ferridoxin-NADP+ reductase is a major component of antioxidant enzymes (Lee et al., 2006; Michalowski et al., 1989; Montricharda et al., 2009), and SOD activity is associated with salt tolerance of tomato (Koca et al., 2006). Based on results from those previously reported and

the current studies, we hypothesize that a mechanism for controlling oxidative stress involves the induction of SOD and ferridoxin-NADP+ reductase, which would lead to higher antioxidant capacity in *S. chilense*.

In *S. chilense*, Q-cytochrome C reductase in the oxidative phosphorylation pathway and three key photorespiratory enzymes (phosphoglycolate phosphatase, hydroxypyruvate reductase, and glycolate oxidase) were suppressed by salt stress. Reduced activity of these enzymes should generate a lesser amount of ROS. Additionally, the glyoxylate bypass was induced. Activation of this pathway avoids the oxidative phases of the Kreb's cycle, thus providing an additional means to reduce the potential damage of the oxidative burst to cells (Kelly et al., 2002).

We conclude *S. chilense* could have mobilized two mechanisms to control oxidative stress and the resultant cellular damage: by enhancing the antioxidant enzymatic system and reducing the generation of ROS.

MECHANISM FOR REDUCING ION TOXICITY. When plants are grown under saline condition, accumulation of excessive amounts of Na+ in the cytoplasm is toxic to plant cells. Plants can enhance salt tolerance through activation of a selective ion transport system to maintain Na+ homeostasis in the cytosol (Maeshima, 2000, 2001; Zhu, 2003). In *S. chilense*, vacuolar ATPases and vesical transport proteins were affected by salt stress. These proteins are responsible for selective uptake, sequestration, and compartmentalization of toxic ions. Genes encoding for these proteins should be investigated for their role in salt tolerance in tomato.

Additionally, high concentration of sodium ions (Na+) causes ionic stress as a result of solute imbalances and osmotic stress that reduces water availability (Silva and Gerós, 2009). Porins are defined as water-filled channels through which

Table 5. Salt-suppressed proteins in root of *Solanum chilense*.

Spot no.	Fold change value[z]	P[y]	UniGene code[x]	Putative protein	Peptide sequence hit[w]	Protein score[v]
Proteases						
765	−1.8	0.012	SGN-U562601	Peptidase M1 family protein	IGGGVNIPR	180
732	−1.5	0.007	SGN-U590104	Proteasome subunit beta type 1	DIYTGDKLEIVVLNADGIR	40
Transporters						
514	−1.8	0.009	SGN-U588197	Vesical transport v-SNARE 12	ISPSPIIR	26
630	−2.3	0.003	SGN-U588197	Vesical transport v-SNARE 12	ISPSPIIR	26
532	−2.3	3.65E-04	SGN-U582450	Germin-like protein	HIVQGEVFVFPR; IDYAPGGINPPHLHPR	48
327	−1.6	8.14E-04	SGN-U583085	Peroxidase 12	DSVVLTGGPNYDVPLGR	38
Singal transduction						
686	−3.1	0.002	SGN-U586603	Leucine-rich repeat transmembrane protein kinase	VVSVSIPR	277
Glucose						
531	−3.7	1.83E-04	SGN-U580596	Glucose phosphomutase	TLMVLSMK	95
Malate-aspartate shuttle (TCA cycle)						
312	−1.6	0.005	SGN-U577771	Malate dehydrogenase	MELVDAAFPLLK	204
Other proteins						
761	−1.9	0.001	SGN-U580870	Type I CP29 polypeptide	YQAYELIHAR	36
404	−2	0.006	SGN-U586462	Hypothetical protein	DRLIALR	31

[z]Fold change value is the ratio of the normalized volume of the same spot in the condition of salt-treated (growing in half-strength Hoagland's solution containing 200 mM NaCl for 25 d) versus control (in half-strength Hoagland's solution). For example, a value of 2.0 represents a twofold increase, whereas −2.0 represents a twofold decrease from treated to control conditions.

[y]Probability value in an analysis of variance test of difference between treated and untreated samples each with three biological replicates.

[x]Code for each unigene sequence in the SOL Genomics Network (Ithaca, NY) database.

[w]Peptide sequence used in Mascot (Version 2.3; Matrix Science, Boston, MA) search to identify the protein in the protein database.

[v]Protein score is derived from the ion scores. An ion's score is based on the calculated probability that the observed match between the experimental data and the database sequence is a random event. The reported score is −10Log (P). For a search containing a small number of queries, the protein score is the sum of the highest ions score for each unique sequence, excluding the scores of duplicate matches. A correction (usually very small) is applied to reduce the contribution of low-scoring random matches.

molecules of up to 600 Da may diffuse (Nikaido and Rosenberg, 1981). Their function is to facilitate both passive and selective diffusion of ions and small metabolites across cell membranes (Aljamal et al., 1993; Bölter and Soll, 2001). In the salt-treated root tissues of *S. chilense*, a porin (voltage-dependent anion-selective channel protein) was induced. This type of protein could play a significant role in uptake and redistribution of Na^{+} ions in the root system. However, the unigene SGN-U570210 contains only a partial gene sequence without the signal peptide fragment (SOL Genomics Network, 2011); thus, the organelle localization of this protein could not be predicted nor the exact function of this protein against salt stress in *S. chilense*.

High salt concentrations induce osmotic stress. Production and accumulation of compatible osmolytes and osmoprotectants are two major molecular tolerance mechanisms adopted by plants under salt stress (Lee et al., 2008; Sacher and Staples, 1985). In *S. chilense,* three enzymes including methyltetrahydropteroyltriglutamate-homocysteine methyltransferase, S-adenosylmethionine synthetase 1, and adenosylhomocysteinase (spot 309, 4.3-fold) were induced by the salt treatment in roots. These enzymes are responsible for the regeneration of SAM, which serves as the methyl donor for biosynthesis of compatible osmolytes (Bohnert and Jensen, 1996; Hanson et al., 1995).

Salt stress also induced other enzymes in the SAM regeneration pathway in leaves of *S. chilense* and tomato 'Money Maker' (Zhou et al., 2009). In addition, the induction of osmotin-like protein (spot 669, leaf protein) and betaine-aldehyde dehydrogenase (spot 323, leaf protein) would also enhance the osmoprotection capacity of *S. chilense* plants growing in saline solution.

Taken together, expression of proteins in the osmoprotection and ion transporter categories may facilitate maintaining a stable cellular water status, controlling the uptake of toxic sodium ions from the growth medium into roots and from the apoplastic spaces into leaves, reducing toxic ion concentration in the cytosolic spaces, and ameliorating osmotic stress.

PARTITIONING OF METABOLITES AND SALT STRESS. Under environmental stress, the metabolite homeostasis can be disrupted in susceptible plants. Metabolic adjustments are very important for maintaining normal cellular function in tolerant species. In *S. chilense,* ketol-acid reductoisomerase was induced by salt stress in both leaves and roots. Ketol-acid reductoisomerase is a key enzyme in the biosynthesis of branched-chain amino acids (BCAAs), pantothenate, and coenzyme A. BCAAs participate in multiple pathways such as peptide elongation, energy regeneration, glutamate recycling, branched-chain ester formation,

and branched-chain fatty acid synthesis. Ketol-acid reductoisomeras is one of the key enzymes that determine the leaf content of BACC in transgenic tomato (Kochevenko and Fernie, 2011, and references therein). In this study, the induction of ketol-acid reductoisomerase in *S. chilense* provided the first evidence for a possible connection between BACC and salt tolerance.

The second metabolic alteration induced by salt stress is the catabolism of glucose. In both roots and leaves, the UDP–glucose pyrophosphorylase was induced. This enzyme catalyzes the reaction that converts glucose into UDP-glucose, which can then be used for the biosynthesis of sucrose and polysaccharides (cell wall or starch). In root tissues, salt induced expression of triose phosphate isomerase, enolase, and NAD-dependent glyceraldehyde-3-phosphate dehydrogenase. The three enzymes are in the glycolytic pathway where glucose is converted into pyruvate, ATP, and NADPH. The elevated activities of these two glucose-consuming pathways could lead to a reduced glucose level in salt-treated tissues. Coincidently, the expression of glucose-dependent glucose phosphomutase was suppressed in roots, which was an indication of a low level of cellular glucose. In a study by Sacher and Staples (1985), the concentration of glucose had a more dramatic elevation in response to salt treatment in salt-susceptible tomato than in tolerant genotypes. These results indicate that low glucose contents could be used as screening criteria for salt tolerance in tomato.

PROTEINS ASSOCIATED WITH CARBON FIXATION AND CARBOHYDRATE METABOLIC PATHWAYS AND THEIR POSSIBLE ROLES IN SALT TOLERANCE. Photosynthesis is the primary pathway for the production of carbohydrates, which are essential for cell growth and proliferation. The capability of a plant to maintain stable photosynthetic rates is significant for sustaining plant growth under saline conditions. In this study, several enzymes in the Calvin cycle were identified; they are the salt-induced GAPDH and ribulose-phosphate 3-epimerase and the salt-suppressed sedoheptulose-1, 7-bisphosphatase (SBPase). Enzymes such as PGK, adolase and transketolase, Rubisco activase, and transketolase were identified in multiple isoforms. Photosynthesis is sensitive to small reductions (20% to 30% less) in the activity of enzymes such as transketolase and SBPase (Lefebvre et al., 2005, and references therein). Thus, salt-induced suppression of SBPase could have a significant and negative impact on photosynthesis of *S. chilense*. On the other hand, salt also suppressed enzymes in the photorespiration pathway. Photorespiration can significantly reduce the efficiency of carbon fixation (20% to 40%) in photosynthesis in C3 plants such as tomato (Sharkey, 1988). In the salt-tolerant species such as *S. chilense*, the suppression of photorespiratory enzymes could lead to lower activity of the photorespiratory pathway, which may be a mechanism to compensate for the low net photosynthetic rates when plants are growing in a saline solution.

Enzymes such as PGK and adolase occur in chloroplasts and in the cytosol of higher plants. These enzymes catalyze different reactions depending on their cellular locations. The chloroplast PGK isoenzyme participates in the Calvin cycle, and the cytosolic enzyme is involved in glycolysis (Anderson et al., 2004; Nowitzki et al., 2004). In *S. chilense*, two isoforms (spot 492 with higher pI value and spot 780 at lower pI) were identified; the former was induced and the latter one was suppressed by the salt stress.

Similar to PGK, higher plants also have two forms of aldolase: cytoplasmic (AldC) and plastidic (AldP) (Gasperini

and Pupillo, 1982; Valenti et al., 1987). AldC and AldP are involved in different metabolic pathways and catalyze the same reaction but in opposite directions from each other. The cytoplasmic aldolase (AldC, higher pI) has an important role in the production of ATP by stimulating glycolysis. AldP is involved in the photosynthetic carbon reduction cycle; expression of the *AldP* gene is affected by salt stress in tobacco (*Nicotiana tabacum*) (Haake et al., 1998; Yamada et al., 2000). In salt-treated *S. chilense*, two adolase protein spots with higher pI values were induced (spots 569, 585) whereas three spots of lower pI values (spots 559, 563, 931) were suppressed. It is very important to identify the subcellular localization of these isoforms to reveal the role of these enzymes in salt tolerance. Future studies should focus on comparing organelle-specific sub-proteomes combined with metabolite profiling.

Literature Cited

Ahn, J.C., D.W. Kim, Y.N. You, M.S. Seok, J.M. Park, H. Hwang, B.G. Kim, S. Luan, H.S. Park, and H.S. Cho. 2010. Classification of rice (*Oryza sativa* L. Japonica nipponbare) immunophilins (FKBPs, CYPs) and expression patterns under water stress. BMC Plant Biol. doi: 10.1186/1471-2229–0-253.

Alban, A., S.O. David, L. Bjorkesten, C. Andersson, E. Sloge, S. Lewis, and I. Currie. 2003. A novel experimental design for comparative two-dimensional gel analysis: Two-dimensional difference gel electrophoresis incorporating a pooled internal standard. Proteomics 3:36–44.

Aljamal, J.A., G. Genchi, V. De Pinto, L. Stefanizzi, A. De Santis, R. Benz, and F. Palmieri. 1993. Purification and characterization of porin from corn (*Zea mays* L.) mitochondria. Plant Physiol. 102:615–621.

Anderson, L.E., J.A. Bryant, and A.A. Carol. 2004. Both chloroplastic and cytosolic phosphoglycerate kinase isozymes are present in the pea leaf nucleus. Protoplasma 223:103–110.

Bai, Y. and P. Lindhout. 2007. Domestication and breeding of tomatoes: What have we gained and what can we gain in the future? Ann. Bot. (Lond.) 100:1085–1094.

Balibrea, M.E., J. Dell'Amico, M.C. Bolarín, and F. Pérez-Alfocea. 2000. Carbon partitioning and sucrose metabolism in tomato plants growing under salinity. Physiol. Plant. 110:503–511.

Bohnert, H.J. and R.G. Jensen. 1996. Strategies for engineering water-stress tolerance in plants. Trends Biotechnol. 14:89–97.

Bölter, B. and J. Soll. 2001. Ion channels in the outer membranes of chloroplasts and mitochondria: Open doors or regulated gates? EMBO J. 20:935–940.

Borsani, O., J. Cuartero, J.A. Fernández, V. Valpuesta, and M.A. Botella. 2001. Identification of two loci in tomato reveals distinct mechanisms for salt tolerance. Plant Cell 13:873–887.

Bouché, N. and H. Fromm. 2004. GABA in plants: Just a metabolite? Trends Plant Sci. 9:110–115.

Cuartero, I., M.C. Bolarín, M.J. Asíns, and V. Moreno. 2006. Increasing salt tolerance in the tomato. J. Expt. Bot. 57:1045–1058.

Dehan, K. and M. Tal. 1978. Salt tolerance in the wild relatives of the cultivated tomato: Responses of *Solanum pennellii* to high salinity. Irrig. Sci. 1:71–76.

Dillon, S.L., F.M. Shapter, R.J. Henry, G. Cordeiro, L. Izquierdo, and L.S. Lee. 2007. Domestication to crop improvement: Genetic resources for *Sorghum* and *Saccharum* (Andropogoneae). Ann. Bot. (Lond.) 100:975–989.

Flowers, T.J., P.F. Troke, and A.R. Yeo. 1977. The mechanism of salt tolerance in halophytes. Annu. Rev. Plant Physiol. 28:89–121.

Flowers, T.J. and A.R. Yeo. 1995. Breeding for salinity resistance in crop plants: Where next? Aust. J. Plant Physiol. 22:875–884.

Food and Agriculture Organization of the United Nations. 2008. FAO land and plant nutrition management service. 3 Jan. 2011. <http://www.fao.org/ag/agl/agll/spush/>.

Gasperini, C. and P. Pupillo. 1982. Aldolase isozymes of maize leaves. Plant Sci. Lett. 28:163–171.

Göthel, S.F. and M.A. Marahiel. 1999. Peptidyl-prolyl cis-trans isomerases, a superfamily of ubiquitous folding catalysts. Cell. Mol. Life Sci. 55:423–436.

Haake, V., R. Zrenner, U. Sonnewald, and M. Stitt. 1998. A moderate decrease of plastid aldolase activity inhibits photosynthesis, alters the levels of sugars and starch, and inhibits growth of potato plants. Plant J. 14:147–157.

Hanson, A.D., J. Rivoal, M. Burnet, and B. Rathinasabapathi. 1995. Biosynthesis of quaternary ammonium and tertiary sulphonium compounds in response to water deficit, p. 189–198. In: Smirnoff, N. (ed.). Environment and plant metabolism: Flexibility and acclimation. Bios Scientific, Oxford, UK.

Hanson, B.R., D.E. May, J. Simnek, J.W. Hopmans, and R.B. Hutmacher. 2009. UC Davis drip irrigation provides the salinity control needed for profitable irrigation of tomatoes in San Joaquin Valley. Calif. Agr. 63:131–136.

Hoagland, D.R. and D.I. Arnon. 1950. The water-culture method for growing plants without soil. California Agr. Expt. Sta. Circ. 347.

Ivery, M.T. 2000. Immunophilins: Switched on protein binding domains? Med. Res. Rev. 20:452–484.

Karp, N.A. and K.S. Lilley. 2007. Design and analysis issues in quantitative proteomics studies. Proteomics 7(suppl 1):42–50.

Karp, N.A., P.S. McCormick, M.R. Russell, and K.S. Lilley. 2007. Experimental and statistical considerations to avoid false conclusions in proteomics studies using differential in-gel electrophoresis. Mol. Cell. Proteomics 6:1354–1364.

Kelly, B.G., D.M. Wall, C.A. Boland, and W.G. Meijer. 2002. Isocitrate lyase of the facultative intracellular pathogen Rhodococcus equi. Microbiology 148:793–798.

Koca, H., F. Ozdemir, and I. Turkan. 2006. Effect of salt stress on lipid peroxidation and superoxide dismutase and peroxidase activity of Lycopersicon esculentum and L. pennellii. Biol. Plant. 50:745–748.

Kochevenko, A. and A.R. Fernie. 2011. The genetic architecture of branched-chain amino acid accumulation in tomato fruits. J. Expt. Bot. doi: 10.1093/jxb/err091.

Lambers, H. 2003. Introduction to dryland salinity. A key environmental issue in southern Australia. Plant Soil 257:5–7.

Lee, G., R.N. Carrow, R.R. Duncan, M.A. Eiteman, and M.W. Rieger. 2008. Synthesis of organic osmolytes and salt tolerance mechanisms in Paspalum vaginatum. Environ. Exp. Bot. 63:19–27.

Lee, Y., S. Peña-Llopis, Y.S. Kang, H.D. Shin, B. Demple, E.L. Madsen, C.O. Jeon, and W. Park. 2006. Expression analysis of the fpr (ferredoxin-NADP+ reductase) gene in Pseudomonas putida. KT2440. Biochem. Biophys. Res. Commun. 339:1246–1254.

Lefebvre, S., T. Lawson, O.V. Zakhleniuk, J.C. Lloyd, C.A. Raines, and M. Fryer. 2005. Increased sedoheptulose-1, 7-bisphosphatase activity in transgenic tobacco plants stimulates photosynthesis and growth from an early stage in development. Plant Physiol. 138:451–460.

Maeshima, M. 2000. Vacuolar H (+)-pyrophosphatase. Biochim. Biophys. Acta 1465:37–51.

Maeshima, M. 2001. Tonoplast transporters: Organization and function. Annu. Rev. Plant Physiol. Plant Mol. Biol. 52:469–497.

Maggio, A., G. Raimondi, A. Martino, and S. De Pascale. 2007. Salt stress response in tomato beyond the salinity tolerance threshold. Environ. Exp. Bot. 59:276–282.

Michalowski, C.B., J.M. Schmitt, and H.J. Bohnert. 1989. Expression during salt stress and nucleotide sequence of cDNA for ferredoxin-NADP+ reductase from Mesembryanthemum crystallinum. Plant Physiol. 89:817–822.

Mittova, V., M. Tal, M. Volokita, and M. Guy. 2002. Salt stress induces up-regulation of an efficient chloroplast antioxidant system in the salt-tolerant wild tomato species Lycopersicon pennellii but not in the cultivated species. Physiol. Plant. 115:393–400.

Montricharda, F., F. Alkhalfiouib, H. Yanoc, W.H. Venseld, W.J. Hurkmand, and B.B. Buchanane. 2009. Thioredoxin targets in plants: The first 30 years. J. Proteomics 72:452–474.

Nigg, E.A. 1993. Cellular substrates of p34cdc2 and its companion cyclin-dependent kinases. Trends Cell Biol. 3:296–301.

Nikaido, H. and E.Y. Rosenberg. 1981. Effect on solute size on diffusion rates through the transmembrane pores of the outer membrane of Escherichia coli. J. Gen. Physiol. 77:121–135.

Nowitzki, U., G. Gelius-Dietrich, M. Schwieger, K. Henze, and W. Martin. 2004. Chloroplast phosphoglycerate kinase from Euglena gracilis endosymbiotic gene replacement going against the tide. Eur. J. Biochem. 271:4123–4131.

Pang, C.H. and B.S. Wang. 2008. Oxidative stress and salt tolerance in plants. Prog. Bot. 69:231–245.

Postel, S. 1989. Water for agriculture: Facing the limits. Worldwatch paper 93. Worldwatch Institute, Washington, DC.

Rengasamy, P. 2006. World salinization with emphasis on Australia. J. Expt. Bot. 57:1017–1023.

Rick, C.M. 1988. Tomato-like nishshades—Affinities, autoecology, and breeders opportunities. Econ. Bot. 42:145–154.

Rick, C.M. 1991. Tomato genetic resources of South America reveal many genetic treasures. Diversity 7:54–56.

Sacher, R.F. and R.C. Staples. 1985. Inositol and sugars in adaptation of tomato to salt. Plant Physiol. 77:206–210.

Sánchez, N.S., R. Arreguín, M. Calahorra, and A. Peña. 2008. Effects of salts on aerobic metabolism of Debaryomyces hansenii. FEM. Yeast Res. 8:1303–1312.

Schonbrunner, E.R. and F.X. Schmid. 1992. Peptidyl-prolyl cis-trans isomerase improves the efficiency of protein disulfide isomerase as a catalyst of protein folding (oxidative folding/cyclophilfin/ribonudease T1). Proc. Natl. Acad. Sci. USA 89:4510–4513.

Sharkey, T. 1988. Estimating the rate of photorespiration in leaves. Physiol. Plant. 73:147–152.

SOL Genomics Network. 2011. SOL Genomics Network. 3 Jan. 2011. <http://solgenomics.net/search/unigene.pl?unigene_id=SGN-/>.

Sidari, M., C. Mallamaci, and A. Muscolo. 2008. Drought, salinity and heat differently affect seed germination of Pinus pinea. J. For. Res. 13:326–330.

Silva, P. and H. Gerós. 2009. Regulation by salt of vacuolar H+-ATPase and H+-pyrophosphatase activities and Na+/H+ exchange. Plant Signal. Behav. 8:718–726.

Sun, W., X. Xu, H. Zhu, A. Liu, L. Liu, J. Li, and X. Hua. 2010. Comparative transcriptomic profiling of a salt-tolerant wild tomato species and a salt-sensitive tomato cultivar. Plant Cell Physiol. 51:997–1006.

Tanksley, S.D. and S.R. McCouch. 1997. Seed banks and molecular maps: Unlocking genetic potential from the wild. Science 277:1063–1066.

Valenti, V., P. Pupillo, and S. Scaglirini. 1987. Compartmentation of aldolase isoforms in maize leaves. J. Expt. Bot. 38:1228–1237.

Wang, D., X.F. Li, Z.J. Zhou, X.P. Feng, W.J. Yang, and D.A. Jiang. 2010. Two Rubisco activase isoforms may play different roles in photosynthetic heat acclimation in the rice plant. Physiol. Plant. 139:55–67.

Wichelns, D. 1999. An economic model of waterlogging and salinization in arid regions. Ecol. Econ. 30:475–491.

Xing, S.G., Y.B. Jun, Z.W. Hau, and L.Y. Liang. 2007. Higher accumulation of gamma-aminobutyric acid induced by salt stress through stimulating the activity of diamine oxidases in Glycine max (L.) Merr. roots. Plant Physiol. Biochem. 45:560–566.

Yamada, S., T. Komori, A. Hashimoto, S. Kuwata, H. Imaseki, and T. Kubo. 2000. Differential expression of plastidic aldolase genes in Nicotiana plants under salt stress. Plant Sci. 154:61–69.

Yañez, M., I. Verdugo, M. Rodríguez, S. Prat, and S. Ruiz-Lara. 1998. Highly heterogeneous families of Ty1/copia retrotransposons in the Lycopersicon chilense genome. Gene 222:223–228.

Zhang, H.X. and E. Blumwald. 2001. Transgenic salt tolerant tomato plants accumulate salt in the foliage but not in the fruits. Nat. Biotechnol. 19:765–768.

J. Amer. Soc. Hort. Sci. 136(4):288–302. 2011.

301

Zhang, N., R.P. Kallis, R.G. Ewy, and A.R. Portis, Jr. 2002. Light modulation of Rubisco in *Arabidopsis* requires a capacity for redox regulation of the larger Rubisco activase isoform. Proc. Natl. Acad. Sci. USA 99:3330–3334.

Zhang, S., C.K. Van Pelt, and J.D. Henion. 2003. Automated chip-based nano electrospray-mass spectroscopy for rapid identification of proteins separated by two-dimensional electrophoresis. Electrophoresis 24:3620–3632.

Zhou, S.P., R. Sauve, T. Fish, and T.W. Thannhauser. 2009. Salt induced protein in tomato leaf. J. Amer. Soc. Hort. Sci. 134:289–294.

Zhu, J.K. 2003. Regulation of ion homeostasis under salt stress. Curr. Opin. Plant Biol. 6:441–445.

Zsigmond, L., G. Rigó, A. Szarka, G. Székely, K. Otvös, Z. Darula, K.F. Medzihradszky, C. Koncz, Z. Koncz, and L. Szabados. 2008. *Arabidopsis* PPR40 connects abiotic stress responses to mitochondrial electron transport. Plant Physiol. 146:1721–1737.